scientific reports

Check for updates

OPEN

Extreme events in gene regulatory networks with time-delays

S. Vinoth[1,6], S. Leo Kingston[2]✉, Sabarathinam Srinivasan[3], Suresh Kumarasamy[4,5]✉ & Tomasz Kapitaniak[2]

This work explores distinct complex dynamics of simplified two nodes of coupled gene regulatory networks with multiple delays in two self-inhibitory and mutually activated genes. We have identified the emergence of extreme events within a specific range of system parameter values. A detailed analysis of the time delay-induced emergence of extreme events is illustrated using bifurcation analysis, two-parameter phase diagrams, return maps, temporal plots, and probability density functions. The reasons behind the advent of extreme events are discussed in detail, with possible analogies to simplified two nodes of gene regulatory networks. The occasional large-amplitude bursting originated in the system via interior crisis-induced intermittency, Pomeau-Manneville intermittency, and the breakdown of quasiperiodic intermittency routes. Additionally, we have used various recurrence quantification statistical measures, such as mean recurrence time, determinism, and recurrence time entropy, to describe the transition from periodic or chaotic to unforeseen large deviations. Our approach shows that the sudden surge of variance and mean recurrence time at the transition points can be used as a new metric to detect the critical transitions of distinct extreme bursting events. The comprehensive overview of the interaction between gene regulatory networks, with insights into the formation of unusual dynamics, is beneficial to grasping different neuronal diseases.

Keywords Gene regulatory networks, Time-delay, Extreme events, Recurrence quantification measures

Gene Regulatory Networks (GRNs) have been investigated in living organisms, such as bacteria and viruses since the early 1960s[1]. They remain highly significant in numerous contexts, particularly in the biological and medicinal sciences[2]. Generally, GRNs are described as the network of interactions between DNA, RNA, molecules, and proteins[3,4]. Due to its high connectivity, extreme complexity in its network, and a large variety of genetically pre-coded responses, living organisms can respond to external signals and stimuli[5]. GRNs play a significant role in a considerable number of regular life processes, such as cell differentiation[6], metabolism[7], the cell cycle[8], and signal transduction[9]. For instance, the interaction between proteins and genes forms a network that creates stimuli for the sophisticated biological functions of organisms[3]. The question of how to model or illustrate GRNs in terms of gene functions[3], expression mechanisms[10], and signal-transduction routes[11] remains vague. Mathematical models are beneficial for finding higher-order arrangements of an organism and for accumulating deep understandings of both static and dynamic behaviors of gene networks by extracting functional information from observation data. Hence, considerable measures are utilized to extend mathematical techniques for GRNs research. GRNs can be modeled as networks (undirected or directed), where the nodes represent separate genes, proteins, and so forth, and the edges equal some state of regulation between the nodes[12]. In the literature, gene regulatory networks have been represented in various mathematical forms, including random Boolean networks[13], delay Boolean equations[14], differential equations[15,16], piecewise linear differential equations[17], and stochastic equations[18]. Other approaches also illustrate switch-like and smooth variations in genetic networks, effectively combining discrete and continuous system models[19,20].

From the perspective of modeling *dynamical systems*, the model represents the interactions of gene products, such as mRNAs and proteins, as continuous values. This more precise method enables a thorough understanding of the dynamic nonlinear behavior exhibited by biological systems[21]. Geard et al. reviewed the widespread idea

[1]Center for Nonlinear and Complex Networks, SRM Institute of Science and Technology, Ramapuram, Chennai 600 089, India. [2]Division of Dynamics, Lodz University of Technology, Stefanowskiego 1/15, 90-924 Lodz, Poland. [3]Department of Molecular Analytics, Saveetha School of Engineering, Saveetha Institute of Medical and Technical Sciences (SIMATS), Chennai, Tamilnadu, India. [4]Centre for Artificial Intelligence, Easwari Engineering College, Chennai 600 089, India. [5] Center for Cognitive Science, Trichy SRM Medical College Hospital and Research Center, Trichy, India. [6] Center for Research, SRM TRP Engineering College, Tiruchirappalli, Tamil Nadu, India. ✉email: kingston.cnld@gmail.com; sureshscience@gmail.com

of treating a regulatory network as a dynamical system and described various approaches that have been taken into account for modeling the dynamical system-based GRNs[22]. In addition, genetic regulatory networks with time delays, which are described by functional differential equations or delay differential equations, provide the necessary and sufficient conditions for simplifying the genetic network model and further investigation of the nonlinear properties of the model in terms of local stability and bifurcation, as discussed in Ref.[23]. Furthermore, the time delay between the nodes of a gene regulatory network is a crucial factor to consider, as it significantly influences the processes of transcription, translation, and translocation in genetic networks. In modeling gene regulations, these time delays reflect the slow biochemical reactions between the cytosol and nucleus. Some previous studies in the literature have examined the impact of delay in gene regulatory networks (see Refs:[24–28]).

Various gene circuit motif topologies impacted by time-delay feedback of either positive or negative, as well as a mix of both, have been thoroughly examined in relation to the discrete complex dynamics discussed in Ref.[29]. Subsequently, they disclosed a new intriguing link to connect complex brain illnesses and intense bursting-like events in gene regulatory networks[29]. A single gene with two time-delayed self-regulations, or even two connected genes with time-delayed mutual regulation, can exhibit chaotic behavior. Specifically, the formation of chaotic dynamics generated by delays leads to an aberrant physiological process in the control of genes[30–32]. Upon additional examination of the chaotic zone already present in the GRNs, further examination reveals that the development of unusual bursting dynamics occasionally occurs due to a unique time delay process inside the system[33,34]. The impacts of temporal delays in the self and cross-regulations studied set them apart from earlier reports of chaotic dynamics in gene circuits. The time lags in gene regulation can result from RNA polymerase recruitment, mRNA transport, the translation process via the ribosome, and several other cellular processes.

In general, extreme events are recognized as the occurrence of unforeseen large deviations in the system dynamics for short-living time and eventually return to their bounded motion. These extreme events must be rare, but can appear recurrently at infrequent time intervals. No stick definition exists to confirm the formation of extreme events. Conversely, a widely accepted qualitative measure from the statistical perspective is the so-called significant height threshold (H_s) value that is used to confirm the emergence of extreme events in larger classes of complex dynamical systems[35–37]. This significant height threshold is defined as the sum of the mean and four to eight times the standard deviation of the local maxima of the system variable. In the past few decades, understanding the origin of extreme events (EEs) and their transitions in different disciplines such as hydrodynamics and optical systems[38,39], biological models[40,41], lasers[36,42–44] and complex systems of coupled and network of oscillators[35,37,45] have been studied extensively in the literature. Especially, a deeper understanding of various abnormal events in biological models and gene networks is an appealing problem for understanding various intricate neuronal dynamics. For example, the paradigmatic excitable system of the FitzHugh-Nagumo (FHN) neuron is extensively studied in various aspects: Different topologies of FHN units manifest extreme events that originate via the dynamical process of interior-crisis-induced intermittency[40]. Later, the inclusion of two-time delays in the FHN model exhibits extreme events due to the bubbling transition[46]. A specific local link induced unforeseen extreme events illustrated in ring-coupled FHN systems; besides, the propagation and annihilation of extreme events were explored using various configurations of counter-rotating oscillators[41]. The mitigation of EE using appropriate time-varying interaction parameters is discussed in both coupled and network neuron models[47]. In addition, the time delay effect in the formation and control of extreme events has been reported in a few complex systems[48–50]. However, in this present report, we investigate the formation of extreme events in the simplified two nodes of gene regulatory networks with their possible association with abnormal behavior.

In the literature, various statistical measures have been used to explore complex dynamics, yielding deeper insights into their origins, formation mechanisms, and transitional processes. Among these, recurrence quantification analysis (RQA) is a prominent statistical tool employed to analyze complex real-world data, synthetic data, biological interactions, and sudden transitions[51,52]. Numerous studies have applied RQA to investigate diverse complex dynamics in experimental data[53–55]. For example, the potential of RQA to predict pre-epileptic seizures from electroencephalogram (EEG) data is discussed in Ref.[55]. Additionally, a novel composite approach that combines RQA with Kalman filters has been utilized to monitor and predict bearing degradation processes[53]. Furthermore, Merten et al. demonstrated the presence of instabilities in disk-brake dynamics through RQA analysis of experimental data[56]. In our study, we aim to highlight the advantages of RQA measures, such as determinism (DET), recurrence time entropy (RTE), and mean recurrence time (MRT), in identifying critical transitions that lead to extreme events within our model system. Further details on the various RQA measures and their mathematical formulations can be found in the supplementary material, Section S1.

The recent report by Suzuki et al.[29] explored various complex dynamics in a gene model with time delays, including quasi-periodic, weak chaotic, strong chaotic, and intermittent dynamics. In the absence of time delays, only periodic dynamics can be observed in gene regulatory networks (GRNs). Therefore, understanding the formation of distinct complex dynamics that include time delays is essential for gaining insights into various complicated neurological diseases. For instance, abnormal increases in protein concentrations can contribute to conditions such as Alzheimer's disease, coronary heart disease, and liver failure[57,58]. In our comprehensive analysis of GRNs, we identified the occurrence of intermittent bursting dynamics, which are rare and appear at irregular time intervals. Notably, we discovered that extreme events in GRNs can emerge through three main routes: crisis-induced intermittency, Pomeau-Manneville intermittency, and the breakdown of quasi-periodic intermittency. We performed a range of statistical and dynamical analyses to demonstrate the emergence and transition of these extreme events in two gene circuits, employing both inhibitory and mutually activating strategies.

The paper is organized as follows: the first part describes the mathematical model of two genes that inhibit and activate each other; how these genes can work together in a way that makes sense biologically; and gives a detailed analysis of their stability. Subsequently, we have elaborated on the emergence of different routes to

extreme bursting dynamics and their changeovers under the influence of discrete delay parameters in the system. Next, we discuss the merits of comprehensive statistical measures to identify the distinct intricate dynamics of the gene circuit. In the penultimate section, we examine the impact of noise in gene regulatory networks (GRNs). Finally, in the concluding section, we summarize the key findings of our research.

Gene regulatory model description and stability analysis

In this section, we have presented the mathematical description of the simplified two nodes of the gene regulatory system. Also, we discussed the stability criteria of existing equilibrium states and the formation of periodic dynamics in the system.

System equilibria

The two-gene circuit with two self-inhibitory and mutually activating genes is represented by the following delay differential equations[29]

$$\begin{aligned} \frac{dA(t)}{dt} &= (g_A + g_{AB}B(t-\tau_{12}))\, H^-_{AA}\left[A(t-\tau_1)\right] - k_A A(t), \\ \frac{dB(t)}{dt} &= (g_B + g_{BA}A(t-\tau_{21}))\, H^-_{BB}\left[B(t-\tau_2)\right] - k_B B(t). \end{aligned} \tag{1}$$

Here, A and B represent the protein concentrations measured in nanomolar (nM) units, i.e., 10^{-9} moles per liter. Time (t) is measured in minutes. The protein production rates g_A and g_B are measured in units of nM/minute, and the degradation rates k_A and k_B are measured in units of 1/minute. These units are fixed throughout this work for all simulations. Additionally, the model includes time delay terms in both self-inhibition processes (τ_1 and τ_2) and mutual activation processes (τ_{12} and τ_{21}).

We model gene regulations using Hill functions. The experimental evidence suggests a monotonic sigmoidal-shaped function[59], which increases when $A(t)$ is an activator and decreases when $A(t)$ is an inhibitor. Activating regulation is modeled as $\frac{1}{1+(A_0/A)^n}$, describing a curve that rises from zero and approaches unity. Similarly, inhibitory regulation is represented by the decreasing function $\frac{1}{1+(A/A_0)^n}$. H^-_{AA} and H^-_{BB} are self-inhibitory Hill functions for genes A and B, respectively. These inhibitory Hill functions are expressed as $H^-_{AA}[A(t)] \equiv \frac{1}{1+(A/A_0)^n}$, $H^-_{BB}[B(t)] \equiv \frac{1}{1+(B/B_0)^n}$, where A_0 and B_0 represent the threshold concentrations of the Hill functions, and n represents its rank. Biologically, the Hill coefficient n is related to the molecular binding mechanism. In simple cases, n corresponds to the number of protein monomers required for saturation of binding to the DNA[60].

Equilibrium points

The equilibrium points of the system (1) are obtained by solving the nonlinear equations.

$$k_A A^{n+1} + k_A A_0^n A - g_{AB} A_0^n B - g_A A_0^n = 0, \quad k_B B^{n+1} + k_B B_0^n B - g_{BA} B_0^n A - g_B B_0^n = 0. \tag{2}$$

It is difficult to solve the above equations analytically; hence, we assume $E^*(A^*, B^*)$ be the arbitrary equilibrium point of the system (1) and $A^* > 0$ and $B^* > 0$. In this study, we concentrate on the impact of varying time delays in the model. It is important to note that these time delays do not influence the number of equilibrium points in the model. We have numerically identified all biologically feasible equilibrium points (where A and B represent protein concentrations) and present them in the following section.

Local stability and Hopf bifurcation

To study the local stability and Hopf bifurcation analysis for the system (1), we considered $\tau_1 = \tau_2 = \tau_{12} = \tau_{21} = \tau$ and the Jacobian matrix of the linear model of the system (1) at an arbitrary interior equilibrium point $E^*(A^*, B^*)$ is given by

$$J = \begin{pmatrix} -k_A + a_1 e^{-\lambda\tau} & a_2 e^{-\lambda\tau} \\ a_3 e^{-\lambda\tau} & -k_B + a_4 e^{-\lambda\tau} \end{pmatrix}, \tag{3}$$

where

$$a_1 = -\frac{n\left(\frac{A^*}{A_0}\right)^{n-1}(B^* g_{AB} + g_A)}{A_0\left(\left(\frac{A^*}{A_0}\right)^n + 1\right)^2},\ a_2 = \frac{g_{AB}}{\left(\frac{A^*}{A_0}\right)^n + 1}, a_3 = \frac{g_{BA}}{\left(\frac{B^*}{B_0}\right)^n + 1},\ a_4 = -\frac{n(A^* g_{BA} + g_B)\left(\frac{B^*}{B_0}\right)^{n-1}}{B_0\left(\left(\frac{B^*}{B_0}\right)^n + 1\right)^2}.$$

Then, the characteristic equation is given by

$$\lambda^2 + (k_A + k_B)\lambda + k_A k_B - [(a_1 + a_4)\lambda + (a_1 k_B + a_4 k_A)]e^{-\lambda\tau} + (a_1 a_4 - a_2 a_3)e^{-2\lambda\tau} = 0. \tag{4}$$

Multiplying by $e^{\lambda\tau}$, we get

$$(\lambda^2 + (k_A + k_B)\lambda + k_A k_B)e^{\lambda\tau} - (a_1 + a_4)\lambda - (a_1 k_B + a_4 k_A) + (a_1 a_4 - a_2 a_3)e^{-\lambda\tau} = 0.$$

Then

$$(\lambda^2 + \Omega_1\lambda + \Omega_2)e^{\lambda\tau} - \Omega_3\lambda - \Omega_4 + \Omega_5 e^{-\lambda\tau} = 0. \tag{5}$$

Let $\lambda = i\omega$, separate the real and imaginary parts, and we obtain

$$\left(\Omega_2 + \Omega_5 - \omega^2\right)\cos(\omega\tau) - \Omega_1\omega\sin(\omega\tau) = \Omega_4, \tag{6}$$

$$\Omega_1\omega\cos(\omega\tau) + (\Omega_2 - \Omega_5 - \omega^2)\sin(\tau\omega) = \Omega_3\omega, \tag{7}$$

where $\Omega_1 = k_A + k_B, \Omega_2 = k_A k_B, \Omega_3 = a_1 + a_4, \Omega_4 = a_1 k_B + a_4 k_A, \Omega_5 = a_1 a_4 - a_2 a_3$.

From Eqs. (6) and (7), we obtain

$$\cos(\omega\tau) = \frac{\Omega_4(\Omega_2 - \omega^2 - \Omega_5) + \Omega_1\Omega_3\omega^2}{(\Omega_2 - \omega^2)^2 - \Omega_5^2 + \Omega_1^2\omega^2}, \quad \sin(\omega\tau) = \frac{\Omega_3\omega(\Omega_2 - \omega^2 + \Omega_5) - \Omega_1\Omega_4\omega}{(\Omega_2 - \omega^2)^2 - \Omega_5^2 + \Omega_1^2\omega^2}. \tag{8}$$

Using $\sin^2(\omega\tau) + \cos^2(\omega\tau) = 1$, we get

$$\omega^8 + B_1\omega^6 + B_2\omega^4 + B_3\omega^2 + B_4 = 0, \tag{9}$$

where

$$\begin{aligned}
B_1 &= -4\Omega_2 + 2\Omega_1^2 - \Omega_3^2, \quad B_2 = 6\Omega_2^2 + \Omega_3^2\left(2(\Omega_2 + \Omega_5) - \Omega_1^2\right) - 4\Omega_2\Omega_1^2 - 2\Omega_5^2 + \Omega_1^4 - \Omega_4^2, \\
B_3 &= -4\Omega_2^3 + 2\Omega_3^2\Omega_1^2 + 4\Omega_2\Omega_5^2 - \Omega_3^2(\Omega_2 + \Omega_5)^2 + 2\Omega_2\Omega_4^2 - 2\Omega_5^2\Omega_1^2 + 4\Omega_1\Omega_3\Omega_4\Omega_5 - 2\Omega_5\Omega_4^2 - \Omega_1^2\Omega_4^2, \\
B_4 &= (\Omega_2 - \Omega_5)^2(\Omega_2 + \Omega_5 - \Omega_4)(\Omega_2 + \Omega_5 + \Omega_4).
\end{aligned}$$

Let us assume Eq. (9) has at least one positive root be ω^*, then we obtain the critical value of the time delay, that the system (1) undergoes the Hopf bifurcation given by

$$\tau^* = \frac{1}{\omega^*}\arccos\left(\frac{\Omega_4(\Omega_2 - \omega^{*2} - \Omega_5) + \Omega_1\Omega_3\omega^{*2}}{(\Omega_2^2 - \omega^{*2})^2 - \Omega_5^2 + \Omega_1^2\omega^{*2}}\right). \tag{10}$$

If $\tau = 0$, the characteristic Eq. (4) becomes

$$\lambda^2 - [(a_1 + a_4) - (k_A + k_B)]\lambda + k_A k_B - a_1 k_B + a_4 k_A + a_1 a_4 - a_2 a_3 = 0. \tag{11}$$

It is clear that the system (1) is locally asymptotically stable for $\tau = 0$ if it satisfies

$$(a_1 + a_4) < (k_A + k_B), \quad k_A k_B + a_4 k_A + a_1 a_4 > a_1 k_B + a_2 a_3. \tag{12}$$

Taking the derivative of $\lambda(\tau)$ in Eq. (5) with respect to τ, we get

$$\operatorname{sgn}\left\{\left[\operatorname{Re}\left(\frac{d\lambda(\tau)}{d\tau}\right)^{-1}\right]_{\tau=\tau^*}\right\} = \operatorname{sgn}\left(\operatorname{Re}\left(\frac{\Omega_3}{\lambda\left((\lambda^2 + \Omega_2\lambda + \Omega)\,e^{\lambda\tau} - \Omega_5 e^{-\lambda\tau}\right)} - \frac{\tau}{\lambda}\right)_{\tau=\tau^*}\right) = \operatorname{sgn}\left(\frac{\Omega_3 P_1}{P_1^2 + P_2^2}\right), \tag{13}$$

where

$$P_1 = (\omega^2 - \Omega_2\omega)\sin(\omega\tau) - (\Omega_1\omega^2 + \omega_5)\cos(\omega\tau), \quad P_2 = (-\omega^2 + \Omega_2\omega)\cos(\omega\tau) - (\Omega_1\omega^2 - \Omega_5)\sin(\omega\tau).$$

If **(H1)** $P_1 \neq 0$ holds, then $\operatorname{Re}\left(\frac{d\lambda(\tau)}{d\tau}\right)^{-1}_{\tau=\tau^*} \neq 0$. Based on the above analytical derivations, we can conclude that the system (1) for $\tau \neq 0$ is locally asymptotically stable for $\tau \in (0, \tau^*)$ if it satisfies Eq. (12) and **(H1)**, then the Hopf bifurcation occurs at critical parameter value τ^*.

Result and discussion

We start by looking at the dynamics of GRNs as described in Suzuki (2016) before moving on to the discrete complex dynamics in gene regulatory networks. As an example, we used two gene circuits with two self-inhibitory and mutually activating genes, as shown in Fig. 1a. The brown and blue circles prove a two-gene circuit: the self-activation loops of each gene *A* and *B* contain time-delays τ_1 and τ_2, respectively. Similarly, the time delay among mutual activations of genes is denoted by τ_{21} and τ_{12}. We found interesting dynamics, such as extreme events (in protein concentration), in the gene circuit model when certain system parameters were set to $g_A = 50$, $k_A = 0.20$, $g_B = 50$, $k_B = 0.24$, $g_{AB} = 3.0$, $g_{BA} = 3.00$, $a = 100$, $b = 4$, and a range of different time delays ($\tau_1, \tau_2, \tau_{12}$, and τ_{21}). Throughout this paper, we have fixed the above mentioned constant parameters for all numerical simulations.

The occurrence of steady-state dynamics turns into an oscillatory solution through a Hopf bifurcation for the appropriate time delay value identified in the system. When considering the equality of $\tau_1 = \tau_2 = \tau_{12} = \tau_{21} = \tau$(see Fig. 2(a)), and for a gradual increase of τ within the range of (1.70, 1.85), distinct dynamics of gene regulatory networks (GRNs) are observed, as depicted in Fig. 2b. For $\tau < 1.776$, the model

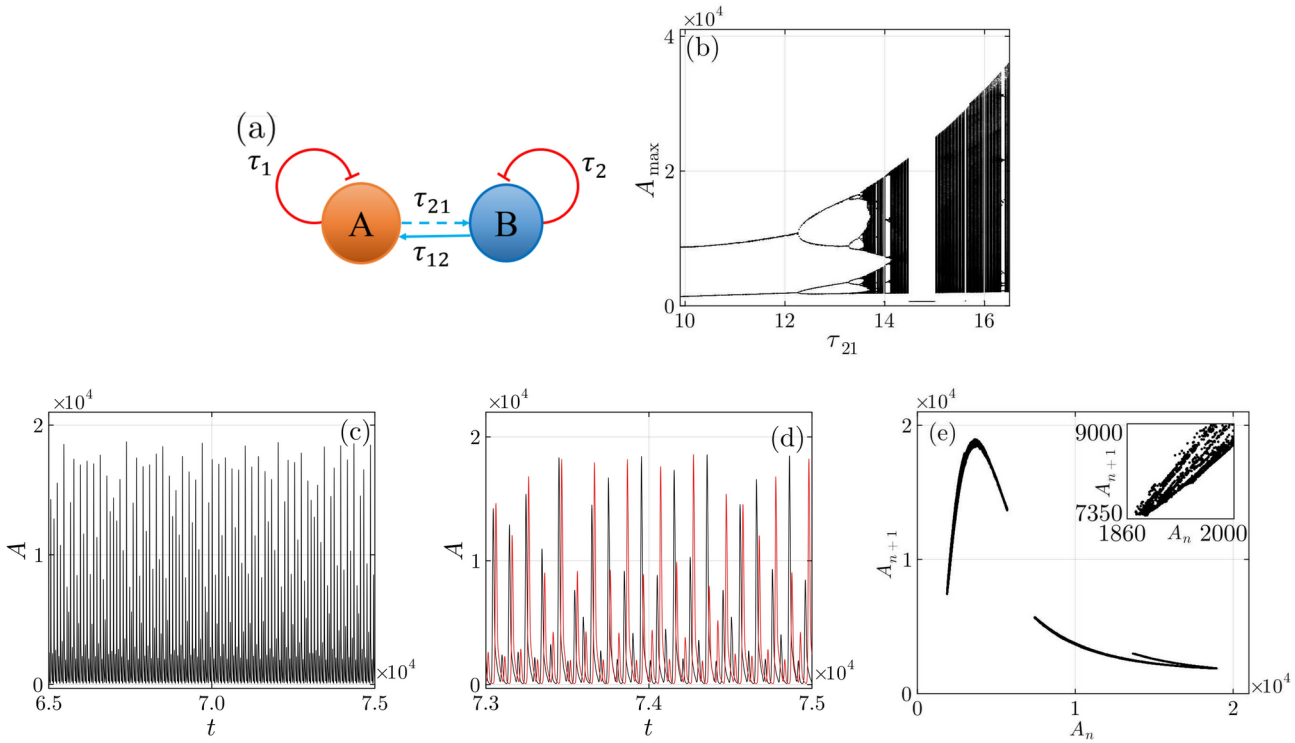

Fig. 1. (**a**) The circuit schematic for the two genes, (A and B), includes fixed self-inhibitory delays (τ_1 and τ_2) and one of the mutually activating delay terms (τ_{12}), indicated by a solid line. Gradually varying τ_{21}(shown as a dashed line) leads to the emergence of chaos through a period-doubling route, as illustrated in the bifurcation diagram in (**b**). The chaotic time series for $\tau_{21} = 13.95$ is presented in (**c**), along with the temporal evaluation of chaotic dynamics for two infinitesimally small initial conditions depicted in (**d**). Additionally, (**e**) displays the return map of the chaotic motion. Other delay parameter values are fixed as $\tau_1 = 6.0$, $\tau_2 = 5.0$, and $\tau_{12} = 7.5$.

exhibits the equilibrium state at $E^*(196.1344, 189.9079)$, which satisfies the condition of Eq. (12), and it is locally asymptotically stable. The phase portrait of asymptotically stable dynamics is pictured in Fig. 2c. On the other hand, at a critical time delay value, i.e., for $\tau^* = 1.776$, we have identified the emergence of oscillatory dynamics from the steady state via Hopf bifurcation. Also, it satisfies the transversality condition $\mathrm{Re}\left(\frac{d\lambda(\tau)}{d\tau}\right)^{-1}_{\tau=\tau^*} \neq 0$. The phase portrait of regular oscillatory dynamics is showcased in Fig. 2d. The analytically obtained formation of the Hopf bifurcation parameter value is plotted as a vertical red line in Fig. 2b that is well matched with the numerical simulation result. Genetic networks often exhibit stable dynamics with multiple fixed points for a wide range of parameter values. However, in this study, we focus on varying the time delay in the model. It is important to note that the time delay does not affect the number of equilibrium points. Also, the proposed model has only one biologically feasible equilibrium point, $E^*(196.1344, 189.9079)$.

Period-doubling route to chaos in GRNs

We began by examining how various dynamics in Gene Regulatory Networks (GRNs) emerge and the impact of the time delay parameter τ_{21} on this process. Fig. 1a illustrates the circuit architecture related to their time delay interactions. To emphasize the significance of the control parameter τ_{21}, we used a dashed line to distinguish it from the other time delay constants. The emergence of strong chaotic dynamics is identified in system eq. (1) via the period-doubling route as we vary the time delay $\tau_{21} = (0, 19)$ and for fixed $\tau_1 = 6.0$, $\tau_2 = 5.0$ and $\tau_{12} = 7.5$. To illustrate different transitions in the system, we have drawn a one-parameter bifurcation diagram for a range of $\tau_{21} \in (10, 17)$. The successive period-doubling routes to chaos are shown in Fig. 1b. Further, with the gradual increase of τ_{21} to the higher values, GRNs manifest chaotic attractors with different amplitudes, that are intercepted by various periodic windows, as illustrated in Fig. 1b. To confirm the presence of chaotic dynamics in the system, we have presented the time series for $\tau_{21} = 13.95$, as shown in Fig. 1c. For further clarification of the chaotic dynamics, we have illustrated the temporal evolution using two infinitesimally small initial conditions, depicted in Fig. 1d. The return map of the chaotic motion is also shown in Fig. 1e, with an inset of magnified region highlighting scattered points that confirm the characteristic features of chaotic dynamics. Upon increasing the $\tau_{21} > 17.0$, the GRNs exhibit rare and recurrent large events, which will be elaborated in the following sections.

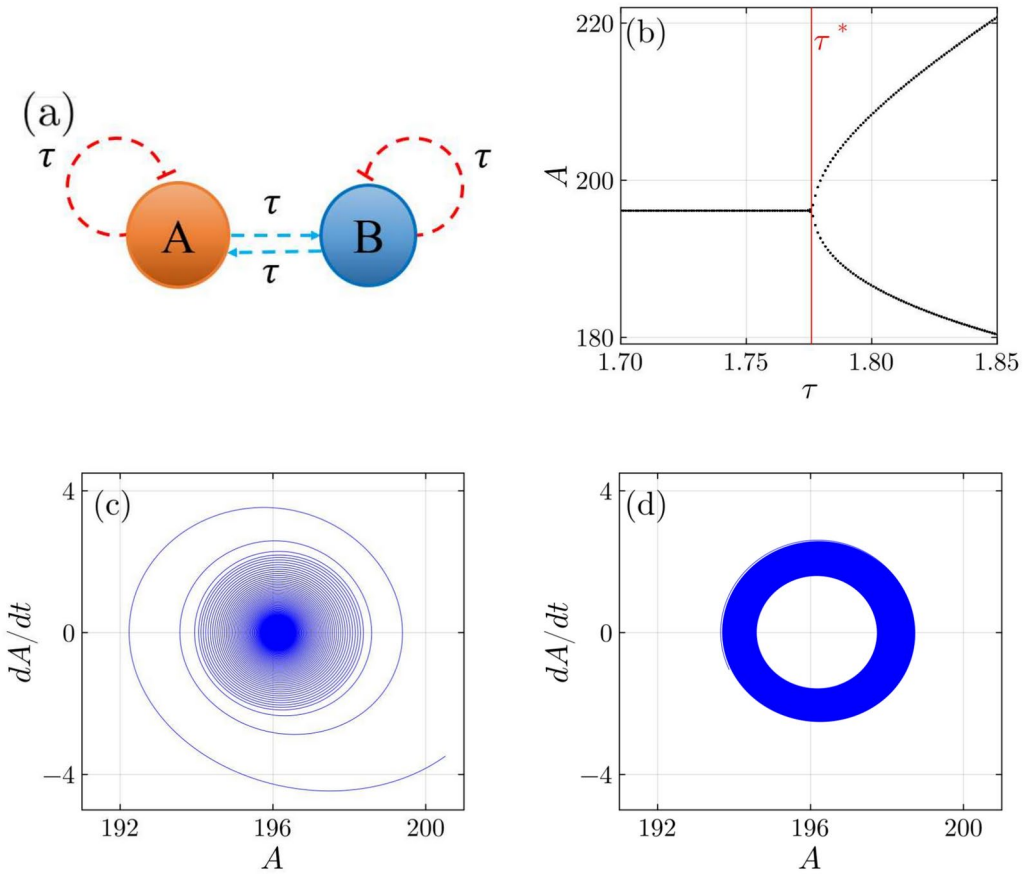

Fig. 2. (**a**) Two gene circuits A and B (represented by orange and blue circles) consist of self-activation τ_1 and τ_2, as well as mutually activation τ_{21} and τ_{12}. In this context, all delay terms are assumed to be equal: $\tau_1 = \tau_2 = \tau_{21} = \tau_{12} = \tau$, and these are illustrated as dashed lines. (**b**) Stability bifurcation diagram for the system Eq. (1) proves the emergence of Hopf bifurcation from the steady state at the critical parameter value of $\tau^* = 1.776$. The vertical red line in (b) elucidates the analytically obtained critical parameter value of the gene model. Phase portraits (**c**) and (**d**) signify the existence of asymptotically stable dynamics and periodic oscillation for the delay parameter values $\tau = 1.75$ and $\tau = 1.776$, respectively.

Extreme event via Pomeau-Manneville intermittency route

Next, we elucidate the formation of extreme events in the protein concentration in the gene regulatory network that originate due to the Pomeau-Manneville (PM) intermittency. Broadly speaking, the Pomeau-Manneville (PM) intermittency transition describes how a system changes from a laminar (periodic) state to a turbulent state under the influence of specific parameters. Within a certain range of control parameter values, the system exhibits periodic motion. As the control parameter continues to increase beyond a critical value, the system remains in this periodic state for extended periods but experiences occasional bursts that disrupt the regular dynamics at finite intervals. As the control parameters increase further, the system ultimately transitions to a fully turbulent state. This entire process is referred to as the Pomeau-Manneville intermittency transition[61]. Here in the GRNs, for the fine-tuning of control parameter τ_{21} from higher to lower values in the range $\tau_{21} \in (19.50, 20.0)$, the system exhibits period two oscillation and extreme events. In order to illustrate a sudden transition from a periodic state to occasional extreme bursting-like events, we have drawn a bifurcation diagram, which is presented in Fig. 3a. The large expansion appears at the critical parameter value $\tau_{21} = 19.878$. We utilized a significant height threshold (H_s) to distinguish extreme events from other dynamics. The significant height values are defined as $H_s = \langle A_n \rangle + n\sigma$, where $\langle A_n \rangle$ represents the mean and σ denotes the standard deviation of the local maxima of A_n. For a different analysis of this work, we fixed n at 6. The obtained threshold values for a range of control parameters are plotted against the bifurcation diagram as a solid red line, as shown in Fig. 3a. For the periodic state, the H_s value is placed above the threshold; conversely, the extreme events surpass the significant height threshold values, which confirms the appearance of rare bursting dynamics in the system.

As previously mentioned, we introduced new statistical measures in the context of extreme events to uncover critical transition points in the gene model that had not been used before. One of these measures is the mean recurrence time (MRT). The MRT was calculated using a significantly larger amount of temporal data. Fig. 3b shows the calculated MRT values for the control parameter τ_{21} within the range (19.50, 20.0). Notably, the MRT elucidates a clear distinction between periodic and extreme event (EE) dynamics. The dashed vertical red line in Fig. 3b indicates the exact change from regular to large bursting dynamics, occurring at $\tau_{21} = 19.878$, which

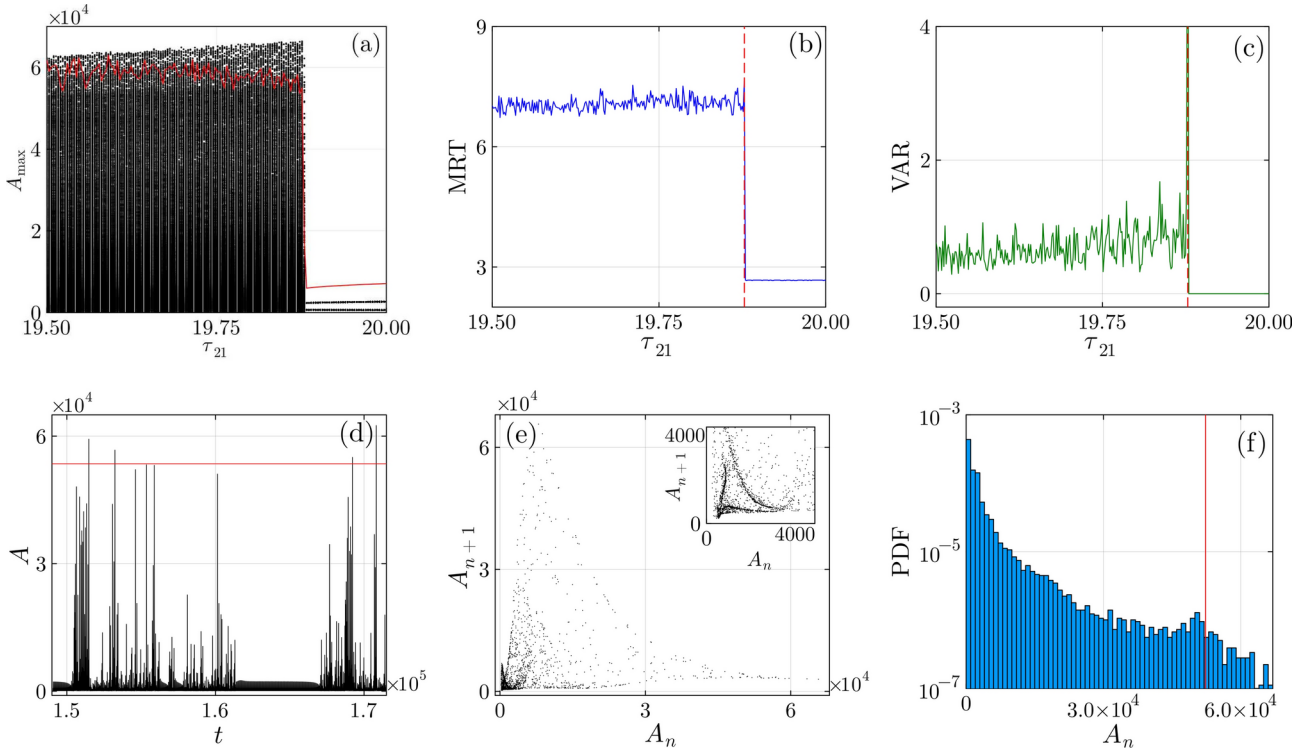

Fig. 3. (**a**) One parameter bifurcation diagram for a range of $\tau_{21} \in (19.5, 20)$ shows the transition to extreme events via the PM intermittency route. The significant height threshold is plotted as a solid red line to discriminate between extreme and non-extreme event domains. Variation of the finite-time MRT in (**b**) and the variance (VAR) measure in (**c**) signifies sudden changes in those values at the critical parameter value. The temporal dynamics of $A(t)$ for $\tau_{21} \approx 19.878$ show sporadic bursting events from the periodic dynamics. The return map for PM intermittent dynamics (**d**) proves occasional bursting from the bounded region (see insert plot for bounded dynamics). The PDF of PM intermittency dynamics (**f**) illustrates a long-tail distribution. The red lines in (**d**) and (**f**) denote the significant height threshold values (H_s).

is marked by a sudden change in values from smaller to larger. Further, the time series indicates that extreme-amplitude protein concentrations are rare events within the network. We want to understand the behavior of the MRT in the context of shorter time frames. This entails examining the variance of the MRT to determine how it fluctuates in smaller intervals in comparison to the entire time series. Insights into the stability and variability of the MRT can be obtained by analyzing the variance, which aids in understanding the underlying dynamics and predictability of these rare extreme events. The variance was calculated by finding the MRT for smaller bins (300 time intervals) within the whole time series used for the MRT calculation. The variance plot for the same range as the MRT analysis is presented in Fig. 3c. As expected, there is no variance for periodic dynamics and moderate variance for extreme bursting dynamics in the gene regulatory networks (GRNs) model. Notably, we identified a significant increase in variance at the critical value of τ_{21}, which supports our MRT analysis. The study demonstrates that MRT and variance analysis can be utilized as effective statistical measures for identifying various critical transitions in complex dynamical systems.

To provide further insight into the creation of rare bursting from the periodic state, we have included a temporal plot in Fig. 3d for $\tau_{21} = 19.878$. Figure 3d makes it evident that the system exhibits rare bursting from the period-two dynamics at irregular time intervals. A return map plot for PM intermittency-induced extreme events is depicted in Fig. 3e. The more concentrated points in the lower amplitude show periodic dynamics, and scatter points appear due to occasional large deviations in the system trajectory. Moreover, we have plotted a probability distribution function (PDF) of extreme events that originated via PM intermittency in Fig. 3f. The PDF plot of Fig. 3f demonstrates the rare probability of occurrence of EEs in the tail region and also reveals a heavy-tail distribution.

Extreme event via quasiperiodic intermittency route

We then focus on investigating the quasiperiodic intermittency (QPI) pathway for the genesis of large amplitude protein concentration. Compared to a large variety of complex dynamical systems, the QPI is an uncommon phenomenon that has been identified in a few models[44,62]. The gene regulatory model exhibits QPI; here, the intermittency emanating from the bounded quasiperiodic motion sporadically also exceeded the significant height threshold value. For a better understanding of the appearance of QPI with extreme events and their transitions, we have presented a one-parameter bifurcation diagram, which is depicted in Fig. 4a. The regular period-two oscillations continue to exist until $\tau_{21} = 20.08$. Upon increasing the $\tau_{21} > 20.08$, the periodic

oscillation shifted to quasiperiodic states via Neimark-Sacker bifurcation[44]. The system persists in quasiperiodic motion for the range of $\tau_{21} \in (20.08, 20.215)$. We can see the transition from periodic to quasiperiodic motion in Fig. 4a. When the control parameter reaches the critical parameter $\tau_{21} \approx 20.216$, the system shows a sudden surge from a bounded quasiperiodic motion into an irregular large amplitude oscillation, say, QPI which is clearly visible in Fig. 4a. The red line in Fig. 4a denotes the significant height threshold that is used to differentiate QPI and other dynamics in the system.

We found the MRT values for the QPI transition for a range of $\tau_{21} \in (20, 21.5)$ using the same methods described in the previous subsection. The results are shown in Fig. 4b. It is clear from the MRT plot that the mean recurrence time values prevail at lower values for the range $\tau_{21} \in (20, 20.215)$. However, the GRNs model witnesses higher MRT values for the range $\tau_{21} \in (20.216, 21.5)$ in that region, where the system manifests rare QPI bursting dynamics. In addition, there is a sudden increase in the MRT value at the critical control parameter value $\tau_{21} = 20.216$, which is also reflected in the variance plot of Fig. 4c. Furthermore, we have identified null variation for the quasiperiodic motion and reasonable fluctuation for the QPI dynamics portrayed in Fig. 4c. The time series plot of quasiperiodic intermittency is presented in Fig. 4d, which manifests the advent of rare bursting from the bounded QP region. Further, to ascertain the QPI dynamics, we have illustrated a return map for $\tau_{21} = 20.216$ in Fig. 4e. It is well obtained from the return map plot (cf. Fig. 4e), the bestrew points reveal the intermittent large expansion that occurred in the system. The magnified plot of Fig. 4e signifies that during the large expansion, the bounded quasiperiodic motion remains the same in the system, resulting in the system exhibiting a closed orbit in the bounded QP motion. Besides, the PDF for QPI dynamics is illustrated in Fig. 4f, proving that a long-tail distribution confirms the appearance of extreme events in the gene circuit model.

So far, we have explored two distinct transitions in the gene regulatory networks (GRNs) that originated from regular (either periodic or quasiperiodic) behavior to rare large amplitude protein concentration within a specific range of τ_{21}. To demonstrate other distinct possibilities for the emergence of extreme dynamics, we have analyzed the system by varying another mutually activated time delay term, τ_1. This analysis is presented in the following sections.

Extreme event via crisis-induced intermittency

In this section, we demonstrate the feasibility of the emergence of extreme bursting dynamics from the chaotic states in the time delay-influenced gene model. For this illustration, we have fixed $\tau_2 = 5.0$, $\tau_{12} = 7.5$, and

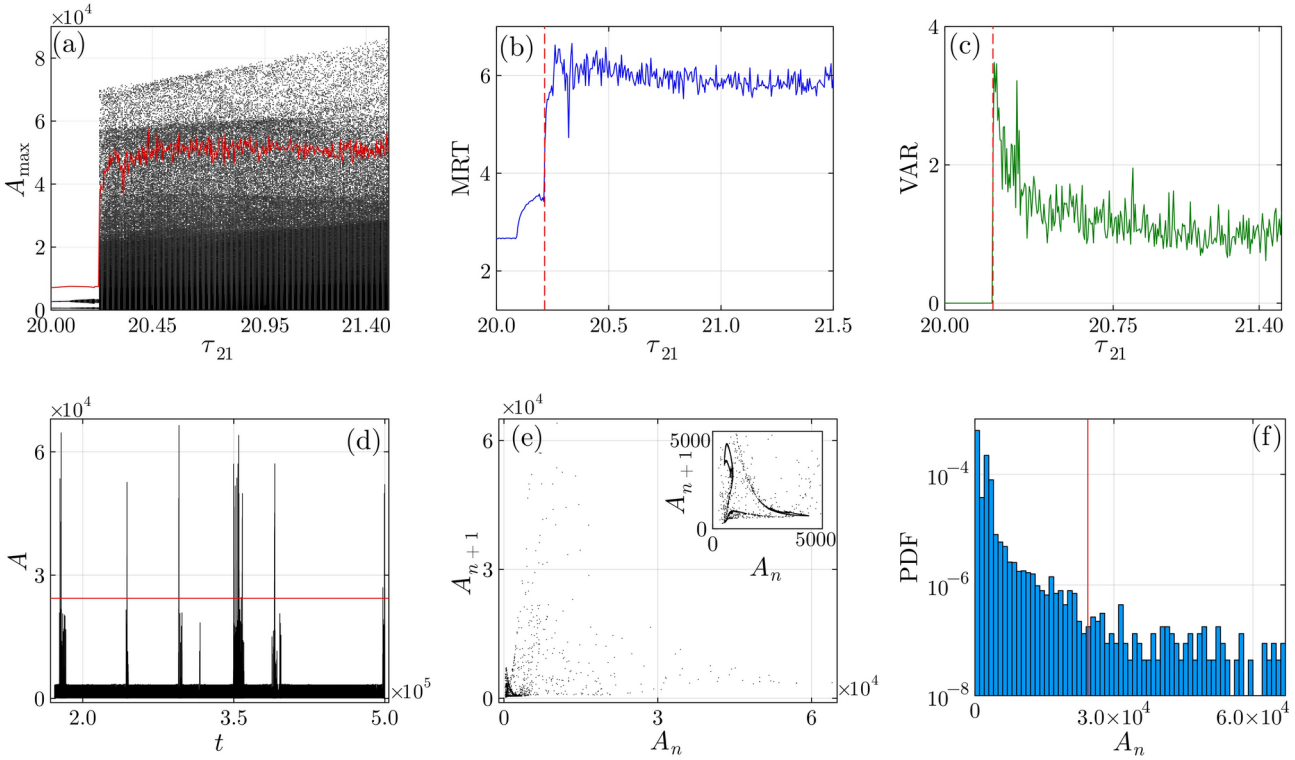

Fig. 4. (**a**) One parameter bifurcation diagram manifests the changeover in the system amplitude from QP to extreme events for a range of $\tau_{21} \in (20, 21.5)$. Significant height threshold values (H_s) are drawn over the bifurcation diagram to discriminate between extreme events and QP dynamics. (**b**) MRT and (**c**) variance (VAR) analysis elucidate the unforeseen shift in their values at the transition point. The time series plot for $\tau_{21} = 20.216$ in (**d**) and the return map in (**e**) illustrate the irregular appearance of bursting dynamics from the bounded QP region. (**f**) The PDF for QPI shows a heavy-tail distribution. The extreme events' qualifier threshold is plotted as a red line in (**d**) and (**f**).

$\tau_{21} = 23.0$. Gradually varying one of the self-inhibitory time delay terms τ_1, the system state variable exhibits occasional large deviations from the bounded chaotic states. The circuit schematic associated with their time delay interaction is shown in Fig. 5a. The solid line in Fig. 5a signifies constant delay, while the dashed line elucidates the control parameter, which is used to pinpoint distinct dynamics in the system. When we slowly change τ_1 in a certain range $\tau_1 \in (6.618, 6.65)$, the gene model shows a series of torus doubling routes. It then moves into bounded chaotic dynamics via the torus breakdown routes[50]. The one-parameter bifurcation diagram is shown in Fig. 5b, which shows that a three-torus forms after period-three oscillations with a critical time delay value of τ_1 about 6.644. Upon decreasing τ_1, the three torus becomes complex QP motion, which is also intercepted by higher-order periodic dynamics. Afterward, the complex QP motion shifted to chaotic dynamics via the torus-breakdown transition, which is inferred from the bifurcation diagram of Fig. 5b.

Subsequently, upon reducing τ_1 to lower values, the gene model proves rare and large amplitude bursting from the bounded chaotic states due to crisis-induced intermittency dynamics. The advent of extreme bursting events from bounded chaotic dynamics is showcased in the bifurcation diagram of Fig. 6a. The sudden increase of system amplitude from the bounded region to approximately eight times larger is apparent from the bifurcation plot (see Fig. 6a). To demarcate the existence of distinct bounded dynamics (periodic, QP, and chaotic) and occasional extreme bursting events, we have calculated the significant height threshold H_s which is plotted as a red line in Fig. 6a. The bursting dynamics in the range of $\tau_1 \in (6.575, 6.611)$, surpass the H_s values, confirming the emergence of extreme events in the system.

Next, we estimate the MRT and its variance for the crisis-induced intermittent transition. The estimated MRT and variance for the range of $\tau_1 \in (6.575, 6.66)$ are depicted in Figs. 6b and c. The gene model exposes constant MRT values for periodic dynamics, and successive increments have been identified for both quasiperiodic and chaotic dynamics. We have observed the only conceivable increase at the transition point, as seen in the MRT plot of Fig. 6b since the system already resides in strong chaos before the sudden large expansion. Nonetheless, the variance plot of Fig. 6c, which shows a sharp rise in value at the crucial parameter value, primarily illustrates it. The vertical dashed line in both Figs. 6b and c indicate the transition point of crisis-induced intermittent bursting dynamics in the gene model. Besides, we have shown the temporal dynamics of $A(t)$ for $\tau_1 = 6.611$ in Fig. 6d which shows the arrival of irregular large bursting dynamics from the bounded chaotic domain. Its equivalent return map shows that sporadic scatter points show the formation of extreme bursting from confined chaotic dynamics (see Fig. 6e) and messy points show the bounded dynamics. For additional confirmation on the appearance of extreme bursting from the chaotic region, the PDF plot is pictured in Fig. 6f. The bounded dynamics reveal a larger probability as compared with the rare existence of extreme bursting in the tail region explicitly revealed in Fig. 6f and the significant height threshold represented as a vertical red line in Fig. 6f. Supplementary section S2 also discusses the emergence of large bursting events influenced by other delay parameters. We were able to find different sudden changes in the system from regular or irregular to occasional large amplitude bursting in the GRNs by using the MRT and variance analysis. In the upcoming section, we will present the details of our use of similar statistical measures to elaborate on the overall picture of the formation of distinct complex dynamics in the system.

Formation of different complex dynamics: influence of delay parameters

The previous sections have shown the three different routes for the formation of extreme bursting events with the impact of a specific delay parameter. In the present section, we show the overall dynamics of the GRNs. We illustrate the system's various intricate dynamics by varying two different time delays with the help of phase diagrams. We have estimated the mean recurrence time for a wider range of delay parameters $\tau_{21} \in (0, 25)$ and $\tau_1 \in (0, 10)$ as shown in Fig. 7a. As we discussed earlier, the MRT measure proves a constant value for regular dynamics, and its values remain lower for periodic states as compared with dissimilar irregular dynamics.

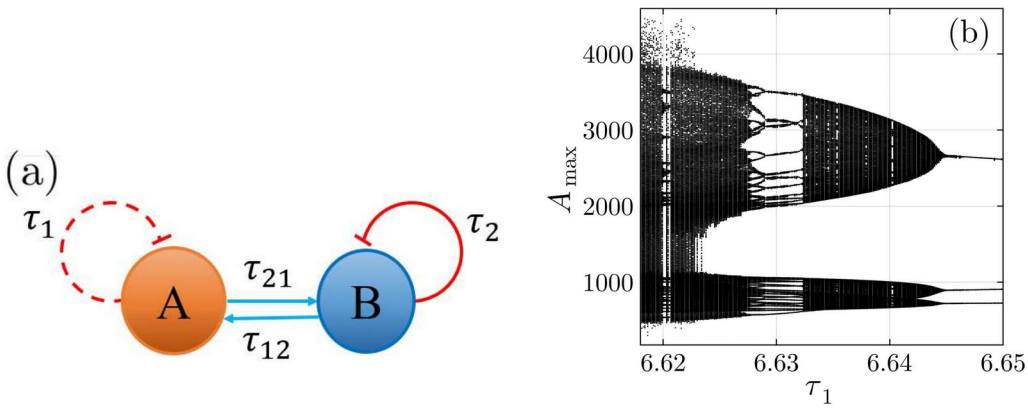

Fig. 5. (**a**) Two-gene (A and B) circuit model with the fixed τ_2, τ_{12}, τ_{21}(solid line) and varying τ_1(dashed line) time delay configuration. (**b**) One parameter bifurcation diagram shows successive torus-doubling dynamics followed by their breakdown to chaos for the range of $\tau_1 \in (6.618, 6.650)$. The remaining delay parameters chosen as $\tau_2 = 5.0$, $\tau_{12} = 7.5$, and $\tau_{21} = 23.0$.

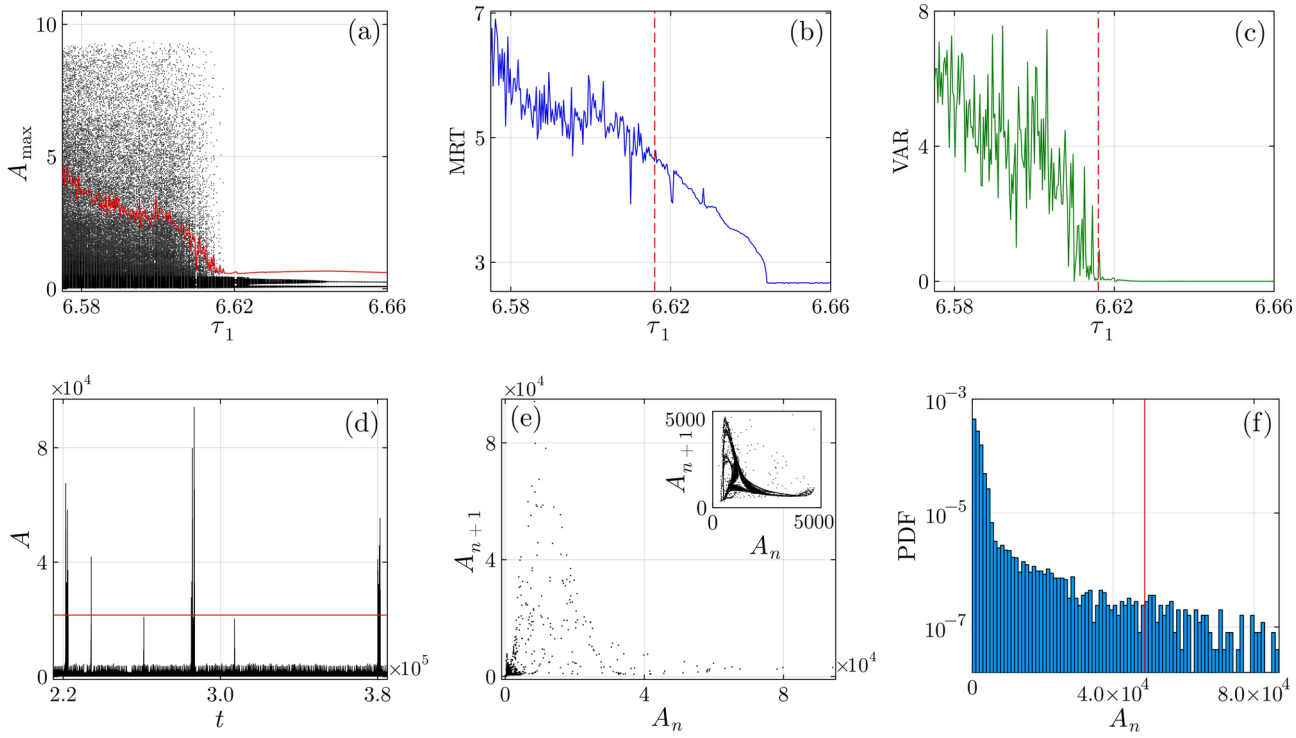

Fig. 6. One parameter bifurcation diagram for $\tau_1 \in (6.575, 6.66)$, shows the advent of EEs from the confined chaotic dynamics at $\tau_1 \approx 6.611$. The significant height threshold is plotted as a solid red line to discriminate between extreme and non-extreme events in a specific range of system parameters. The variation of finite-time MRT and its variance (VAR) are presented in (**b**) and (**c**). The critical transition point is represented as a dashed red line in (**b**) and (**c**) at $\tau_1 = 6.611$. The temporal dynamics of extreme bursting from the chaotic domain (**d**) and their respective return maps (**e**) signify the irregular appearance of EEs from the bounded domain. The PDF of crisis-induced intermittency large expansion manifests the long-tail distribution, exceeding the significant height (H_s - vertical red line) threshold.

Hence, the orange region of Fig. 7a manifests periodic dynamics, whereas the intermingled colors from yellow to purple signify the existence of different complex dynamics. To support this analysis, we have incorporated another reliable statistical measure, so-called determinism (DET). Indeed, this DET measure is used in many classes of nonlinear models to locate the critical transition of the systems[63]. It has been shown that the DET method can help us understand how different nonlinear systems go from having strange nonchaotic dynamics to complex chaotic dynamics[64]. Precisely, the values of DET = 1 denote different periodic dynamics. On the other hand, the lower values of DET signify the advent of discrete, complex dynamics. We used this same approach to discriminate the formation of distinct dynamics in the gene model, and the results are shown in Fig. 7b. It can be inferred from the DET phase diagram of Fig. 7b, that the periodic region (purple) reveals determinism values 1 and lower values (blue to orange) signify the existence of various complex dynamics in GRNs. The DET phase diagram and the MRT analysis also match up well, which supports our observation that we can tell the difference between regular and complex dynamics in the system.

The primary goal of this study is to uncover the formation of distinct, rare, and large-intensity bursts in the GRNs. As a result, we have further classified the region of extreme events from the intermingled complex domain of Figs. 7a and b. We used the variance of MRT to classify extreme and nonextreme regions for the similar parameter space shown in Fig. 7c. The variance analysis adequately identified the existing regions of extreme bursting dynamics, which are visible in the phase diagram of Fig. 7c. Moreover, for additional confirmation to show the extreme bursting domain, we have used the well-established qualifier threshold measure $H_s = \langle A_n \rangle + 6\sigma$ to locate extreme events (EE - black dots) and the nonexistence of extreme events (NEE - white region) dynamics, in the wider parameter region. The outcomes can be seen in Fig.7d, and they support the parameter space for extreme events that we found using variance analysis.

Furthermore, we have evaluated the similar MRT, DET, and variance of MRT for the time delay interaction between τ_{21} and τ_2 regions, which are depicted in Fig. 8. Once again, the MRT and DET statistical measures distinguish periodic (yellow in Fig. 8a and purple Fig. 8b) and non-periodic (intermingled color in both Fig. 8a and b) domains for a broad parameter space, as pictured in Fig. 8a and b. The variance and extreme events' qualifier-based phase diagrams are presented in Fig. 8c and d closely match with one another, which also manifest the formations of extreme events and nonextreme bursting in the specific parameter range. Moreover, we have presented other delays influenced by the formation of different burstings and their statistical analogies elaborated in supplementary section S3. We utilized various recurrent quantification analyses to identify the

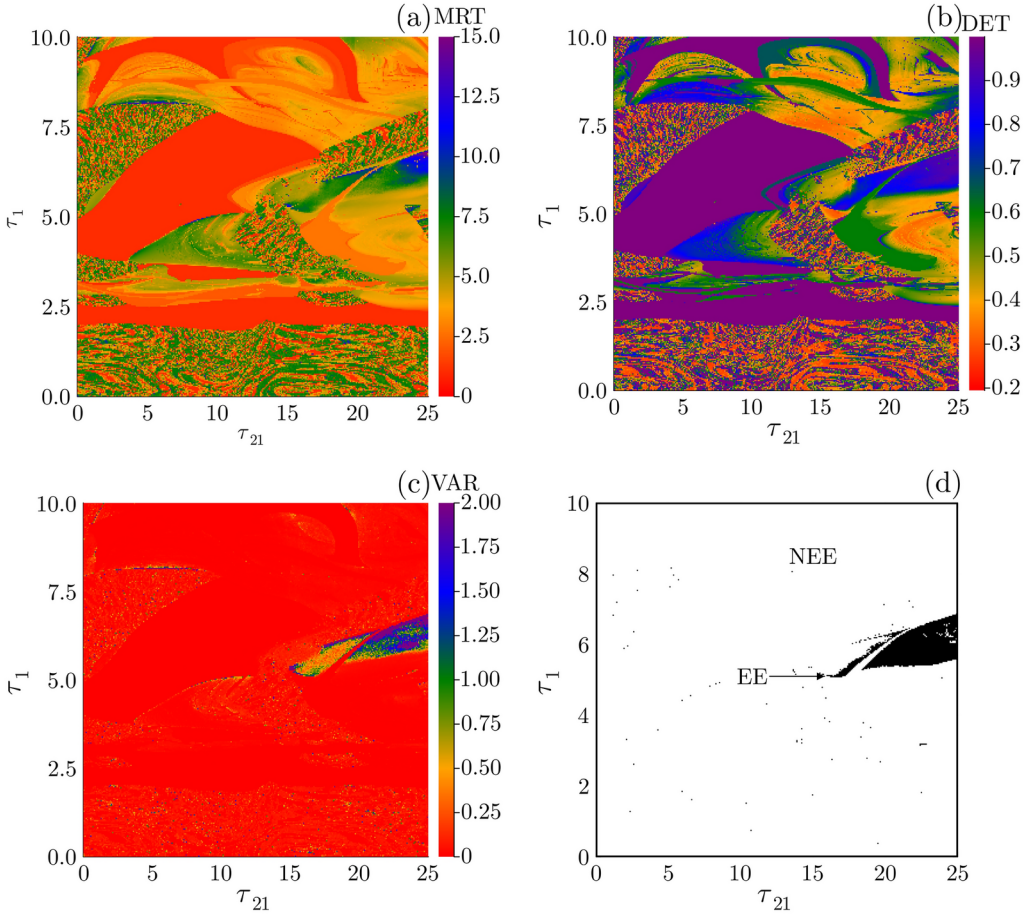

Fig. 7. Phase diagrams for mean recurrence time in (**a**) and determinism in (**b**) at the τ_{21} and τ_1 planes exhibit the formation of distinct complex dynamics in the GRNs. The fixed delay parameters are set as $\tau_2 = 5.0$ and $\tau_{12} = 7.5$. The variance (**c**) and extreme and non-extreme event dynamics (**d**) are shown for a wider parameter region. The higher variance (purple) in (**c**) is well matched with the extreme events domain (black region) in (**d**), revealing the effect of RQA for identifying the critical dynamics domain in the system.

formation of distinct regular and complex dynamics, including extreme events. However, there are limitations to using this measure for determining the distinct stability of gene regulatory networks (GRNs), which is not the primary focus of this study. Additionally, we observed all three different transitions within the selected ranges of $\tau_1, \tau_2, \tau_{12}$, and τ_{21}. It is worth noting that the GRNs exhibit similar transitions for larger values of the different τ parameters, but we did not include those in our discussion to avoid repetition.

Effect of noise

Finally, we evaluated the effect of noise in two simplified gene regulatory networks (GRNs), as certain noise levels are always present in most biological systems. To examine the impact of noise during the transition from a bounded region to unforeseen large amplitude bursting dynamics, we analyzed the quasiperiodic intermittency transitions. The stochastic delay differential equations of the GRNs are expressed as follows:

$$\begin{aligned} \frac{dA(t)}{dt} &= \left(g_A + g_{AB} B(t-\tau_{12})\right) H^-_{AA}\left[A(t-\tau_1)\right] - k_A A(t) + \sigma_A \xi(t), \\ \frac{dB(t)}{dt} &= \left(g_B + g_{BA} A(t-\tau_{21})\right) H^-_{BB}\left[B(t-\tau_2)\right] - k_B B(t) + \sigma_B \xi(t). \end{aligned} \tag{14}$$

In Eq. (14), $\xi(t)$ represents Gaussian white noise with zero mean and unit variance, and σ_A and σ_B denote its relative intensities[11,65]. We set $\sigma_A = \sigma_B = \sigma_d$, and examined the effect of noise in GRNs with different noise intensity values. First, we presented the bifurcation diagram of the quasiperiodic intermittency transition to extreme events for a fixed noise intensity value of $\sigma_d = 0.0001$. The obtained bifurcation diagram (gray points) is plotted in Fig. 9a. For this lower noise intensity, we observed that the GRNs transition from bounded quasiperiodic behavior to extreme events at $\tau_{21} \approx 20.217$. This transition point closely aligns with the quasiperiodic intermittency transition discussed earlier. However, an increase in the noise intensity led to significant changes in system dynamics. For instance, when we set the noise intensity value to $\sigma_d = 0.001$, we found that the system began to display extreme events at $\tau_{21} \approx 20.1$, as illustrated in the bifurcation plot (yellow

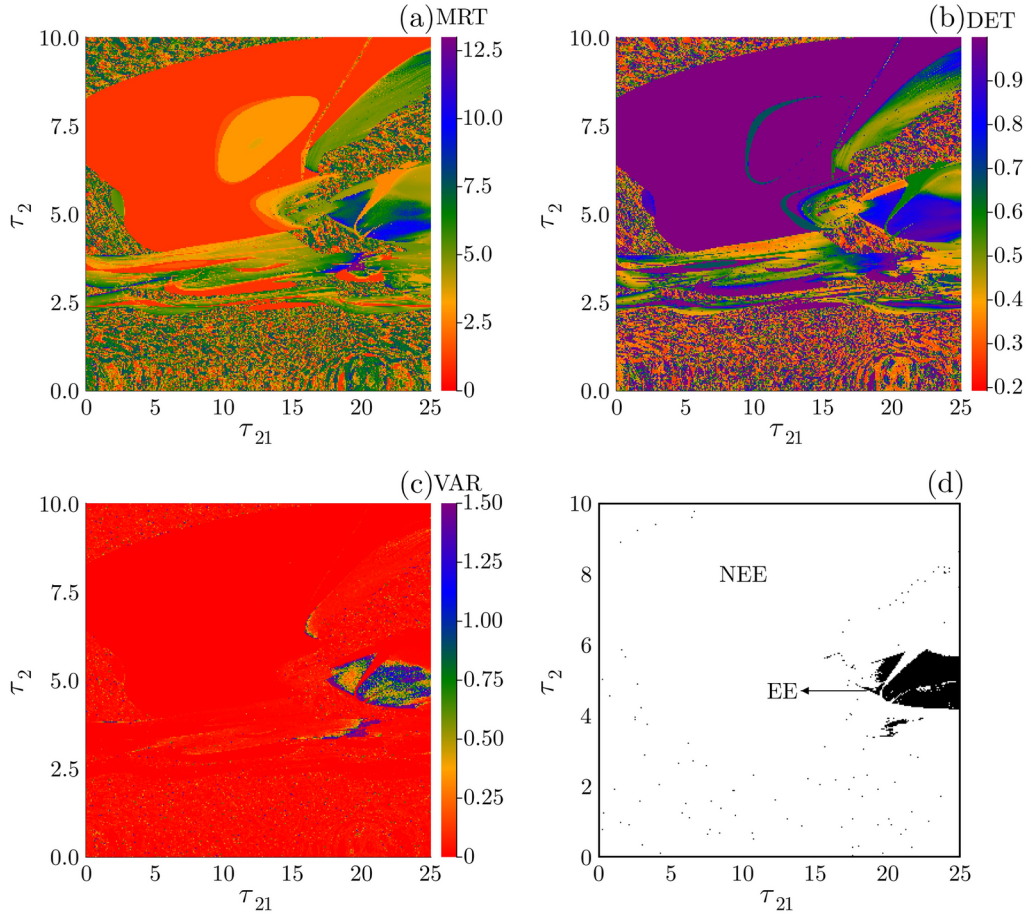

Fig. 8. Phase diagrams: (**a**) mean recurrence time and (**b**) determinism for the range of $\tau_{21} \in (0.0, 25.0)$ and $\tau_1 \in (0.0, 10.0)$ showing the advent of distinct intricate dynamics in the system. Other delay parameters are set as $\tau_1 = 6.0$ and $\tau_{12} = 7.5$. The variance measure (**c**) and extreme and non-extreme event dynamics (**d**) are presented for a wider parameter region. The existence of a higher variance (purple) in (**c**) exactly aligns with the extreme events domain (black region) in (**d**), confirming the rare appearance of extreme bursting events in the system.

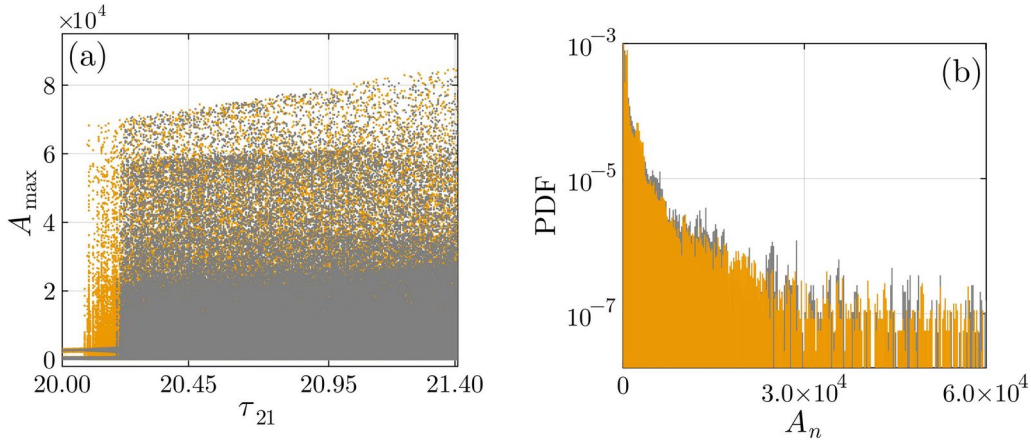

Fig. 9. (**a**) One parameter bifurcation diagram shows quasiperiodic intermittency transition via extreme events with the influence of different noise effects. The GRNs are robust with a lower noise level (gray points: $\sigma_d = 0.0001$) and a significant shift in the transition point with the influence of larger noise strength (yellow point: $\sigma_d = 0.001$). (**b**) The PDF for different noise strengths and τ_{21} values, for $\sigma_d = 0.0001$, $\tau_{21} = 20.217$ (gray), and for $\sigma_d = 0.001$, $\tau_{21} = 20.1$ (yellow), signify the heavy-tail distribution.

points) in Fig. 9a. It is important to note that the two simplified GRNs are resilient to noise at certain levels but exhibit substantial changes after reaching a specific noise intensity threshold. Moreover, to confirm the existence of extreme events at different noise intensities in the GRNs, we depicted the probability distribution function (PDF) for two different σ_d values in Fig. 9b. The PDF reveals a heavy-tailed distribution, confirming the presence of extreme events in the GRNs.

Conclusion

We explored the emergence of diverse dynamical behaviors including periodic, quasiperiodic, chaotic, and extreme bursting patterns in a two-node gene regulatory network influenced by self-inhibitory and mutually activated time-delay parameters. Through a combination of numerical and statistical analyses, such as bifurcation diagrams, return maps, probability distribution functions, mean recurrence time (MRT), and the variance of MRT, we identified the origins, and transitions leading to extreme bursting dynamics and other dynamical phenomena. Our findings highlight that varying time delays in two-node gene regulatory networks reveal a rich spectrum of dynamics, offering valuable insights into the interactions, bursting behaviors, and stability transitions in such systems. The results presented in this work offer several hypotheses and analogies for understanding simple real gene regulatory networks. For example, high-amplitude fluctuations (say EEs) in protein levels can disrupt gene expression, destabilize cellular homeostasis, activate stress responses, and impose a significant metabolic burden that leads to cancer, improper cellular responses, and neurodegenerative diseases[66,67]. Time delays within gene networks are known to influence various biological processes, including delay-induced chaos in circadian gene regulation[29]. Our findings indicate that studying extreme bursting events and chaotic dynamics in simple gene regulatory models, including the impact of delays, can provide valuable insights into understanding how high-amplitude fluctuations emerge and can lead to disrupted gene expression. To expand this research, we plan to construct networks of gene regulatory networks (GRNs) incorporating delays and diverse topological connections. This will enable us to explore the interplay between extreme events and disruptions in circadian rhythms across interconnected pathways in future studies.

Data availability

The datasets generated during the current study are available from the corresponding author on reasonable request.

Received: 31 July 2024; Accepted: 3 April 2025
Published online: 16 April 2025

References

1. Jacob, F. & Monod, J. Genetic regulatory mechanisms in the synthesis of proteins. *J. Mol. Biol.* **3**, 318–356 (1961).
2. Kobayashi, T., Chen, L. & Aihara, K. Modeling genetic switches with positive feedback loops. *J. Theor. Biol.* **221**, 379–399 (2003).
3. Levine, M. & Davidson, E. H. Gene regulatory networks for development. *Proc. Natl. Acad. Sci.* **102**, 4936–4942 (2005).
4. Karlebach, G. & Shamir, R. Modelling and analysis of gene regulatory networks. *Nat. Rev. Mol. Cell Biol.* **9**, 770–780 (2008).
5. Bolouri, H. & Davidson, E. H. Modeling transcriptional regulatory networks. *BioEssays* **24**, 1118–1129 (2002).
6. Drapek, C., Sparks, E. E. & Benfey, P. N. Uncovering gene regulatory networks controlling plant cell differentiation. *Trends Genet.* **33**, 529–539 (2017).
7. Cam, H. et al. A common set of gene regulatory networks links metabolism and growth inhibition. *Mol. Cell* **16**, 399–411 (2004).
8. Chen, L., Wang, R., Kobayashi, T. J. & Aihara, K. Dynamics of gene regulatory networks with cell division cycle. *Phys. Rev. E* **70**, 011909 (2004).
9. Durzinsky, M., Wagler, A. & Marwan, W. Reconstruction of extended petri nets from time series data and its application to signal transduction and to gene regulatory networks. *BMC Syst. Biol.* **5**, 1–17 (2011).
10. MacNeil, L. T. & Walhout, A. J. Gene regulatory networks and the role of robustness and stochasticity in the control of gene expression. *Genome Res.* **21**, 645–657 (2011).
11. Inoue, M. & Kaneko, K. Entangled gene regulatory networks with cooperative expression endow robust adaptive responses to unforeseen environmental changes. *Phys. Rev. Res.* **3**, 033183 (2021).
12. Santillán, M. On the use of the hill functions in mathematical models of gene regulatory networks. *Math. Modell. Nat. Phenomena* **3**, 85–97 (2008).
13. Kauffman, S. A. Metabolic stability and epigenesis in randomly constructed genetic nets. *J. Theor. Biol.* **22**, 437–467 (1969).
14. Ghil, M., Zaliapin, I. & Coluzzi, B. Boolean delay equations: A simple way of looking at complex systems. *Physica D* **237**, 2967–2986 (2008).
15. Mason, J., Linsay, P. S., Collins, J. J. & Glass, L. Evolving complex dynamics in electronic models of genetic networks. *Chaos: Interdiscip. J. Nonlinear Sci.* **14**, 707–715 (2004).
16. Mestl, T., Plahte, E. & Omholt, S. W. A mathematical framework for describing and analysing gene regulatory networks. *J. Theor. Biol.* **176**, 291–300 (1995).
17. Glass, L. Combinatorial and topological methods in nonlinear chemical kinetics. *J. Chem. Phys.* **63**, 1325–1335 (1975).
18. Ramsey, S., Orrell, D. & Bolouri, H. Dizzy: Stochastic simulation of large-scale genetic regulatory networks. *J. Bioinform. Comput. Biol.* **3**, 415–436 (2005).
19. Song, M., Ouyang, Z. & Liu, Z. L. Discrete dynamical system modelling for gene regulatory networks of 5-hydroxymethylfurfural tolerance for ethanologenic yeast. *IET Syst. Biol.* **3**, 203–218 (2009).
20. Ahmad, J., Bernot, G., Comet, J.-P., Lime, D. & Roux, O. Hybrid modelling and dynamical analysis of gene regulatory networks with delays. *Complexus* **3**, 231–251 (2007).
21. Huynh-Thu, V. A. & Sanguinetti, G. Combining tree-based and dynamical systems for the inference of gene regulatory networks. *Bioinformatics* **31**, 1614–1622 (2015).
22. Geard, N. & Willadsen, K. Dynamical approaches to modeling developmental gene regulatory networks. *Birth Defects Res. C. Embryo Today* **87**, 131–142 (2009).
23. Chen, L. & Aihara, K. Stability of genetic regulatory networks with time delay. *IEEE Trans. Circuits Syst. I: Fundamental Theory Appl.* **49**, 602–608 (2002).
24. Wang, Z., Gao, H., Cao, J. & Liu, X. On delayed genetic regulatory networks with polytopic uncertainties: robust stability analysis. *IEEE Trans. Nanobiosci.* **7**, 154–163 (2008).

25. Ribeiro, A., Zhu, R. & Kauffman, S. A. A general modeling strategy for gene regulatory networks with stochastic dynamics. *J. Comput. Biol.* **13**, 1630–1639 (2006).
26. Lou, X., Ye, Q. & Cui, B. Exponential stability of genetic regulatory networks with random delays. *Neurocomputing* **73**, 759–769 (2010).
27. Sun, Q., Xiao, M. & Tao, B. Local bifurcation analysis of a fractional-order dynamic model of genetic regulatory networks with delays. *Neural Process. Lett.* **47**, 1285–1296 (2018).
28. Yu, W., Lu, J., Chen, G., Duan, Z. & Zhou, Q. Estimating uncertain delayed genetic regulatory networks: an adaptive filtering approach. *IEEE Trans. Autom. Control* **54**, 892–897 (2009).
29. Suzuki, Y., Lu, M., Ben-Jacob, E. & Onuchic, J. N. Periodic, quasi-periodic and chaotic dynamics in simple gene elements with time delays. *Sci. Rep.* **6**, 21037 (2016).
30. Zhang, Z. et al. Chaotic motifs in gene regulatory networks. *PLoS ONE* **7**, e39355 (2012).
31. Sevim, V. & Rikvold, P. A. Chaotic gene regulatory networks can be robust against mutations and noise. *J. Theor. Biol.* **253**, 323–332 (2008).
32. Poignard, C. Inducing chaos in a gene regulatory network by coupling an oscillating dynamics with a hysteresis-type one. *J. Math. Biol.* **69**, 335–368 (2014).
33. Bratsun, D., Volfson, D., Tsimring, L. S. & Hasty, J. Delay-induced stochastic oscillations in gene regulation. *Proc. Natl. Acad. Sci.* **102**, 14593–14598 (2005).
34. Gupta, C., López, J. M., Ott, W., Josić, K. & Bennett, M. R. Transcriptional delay stabilizes bistable gene networks. *Phys. Rev. Lett.* **111**, 058104 (2013).
35. Mishra, A. et al. Routes to extreme events in dynamical systems: Dynamical and statistical characteristics. *Chaos: Interdis. J. Nonlinear Sci.* **30**, 063114 (2020).
36. Kumarasamy, S. & Pisarchik, A. N. Extreme events in systems with discontinuous boundaries. *Phys. Rev. E* **98**, 032203 (2018).
37. Chowdhury, S. N., Ray, A., Dana, S. K. & Ghosh, D. Extreme events in dynamical systems and random walkers: A review. *Phys. Rep.* **966**, 1–52 (2022).
38. Onorato, M., Residori, S., Bortolozzo, U., Montina, A. & Arecchi, F. Rogue waves and their generating mechanisms in different physical contexts. *Phys. Rep.* **528**, 47–89 (2013).
39. Dysthe, K., Krogstad, H. E. & Müller, P. Oceanic rogue waves. *Annu. Rev. Fluid Mech.* **40**, 287–310 (2008).
40. Ansmann, G., Karnatak, R., Lehnertz, K. & Feudel, U. Extreme events in excitable systems and mechanisms of their generation. *Phys. Rev. E* **88**, 052911 (2013).
41. Varshney, V., Kumarasamy, S., Mishra, A., Biswal, B. & Prasad, A. Traveling of extreme events in network of counter-rotating nonlinear oscillators. *chaos: An Interdiscip. J. Nonlinear Sci.* **31**, 093136 (2021).
42. Solli, D. R., Ropers, C., Koonath, P. & Jalali, B. Optical rogue waves. *Nature* **450**, 1054–1057 (2007).
43. Pisarchik, A. N., Jaimes-Reátegui, R., Sevilla-Escoboza, R., Huerta-Cuellar, G. & Taki, M. Rogue waves in a multistable system. *Phys. Rev. Lett.* **107**, 274101 (2011).
44. Kingston, S. L., Mishra, A., Balcerzak, M., Kapitaniak, T. & Dana, S. K. Instabilities in quasiperiodic motion lead to intermittent large-intensity events in Zeeman laser. *Phys. Rev. E* **104**, 034215 (2021).
45. Farazmand, M. & Sapsis, T. P. Extreme events: Mechanisms and prediction. *Appl. Mech. Rev.* **71**, 050801 (2019).
46. Saha, A. & Feudel, U. Extreme events in FitzHugh-Nagumo oscillators coupled with two time delays. *Phys. Rev. E* **95**, 062219 (2017).
47. Leo Kingston, S., Kumaran, G., Ghosh, A., Kumarasamy, S. & Kapitaniak, T. Impact of time varying interaction: Formation and annihilation of extreme events in dynamical systems. *Chaos: An Interdiscip. J. Nonlinear Sci.* **33**, 123134 (2023).
48. Zamora-Munt, J., Mirasso, C. R. & Toral, R. Suppression of deterministic and stochastic extreme desynchronization events using anticipated synchronization. *Phys. Rev. E* **89**, 012921 (2014).
49. Mercier, É., Even, A., Mirisola, E., Wolfersberger, D. & Sciamanna, M. Numerical study of extreme events in a laser diode with phase-conjugate optical feedback. *Phys. Rev. E* **91**, 042914 (2015).
50. Kingston, S. L., Kumarasamy, S., Balcerzak, M. & Kapitaniak, T. Different routes to large-intensity pulses in Zeeman laser model. *Opt. Express* **31**, 22817–22836 (2023).
51. Halfar, R., Lawson, B. A., Dos Santos, R. W. & Burrage, K. Recurrence quantification analysis for fine-scale characterisation of arrhythmic patterns in cardiac tissue. *Sci. Rep.* **13**, 11828 (2023).
52. Lopes, M. A. et al. Recurrence quantification analysis of dynamic brain networks. *Eur. J. Neurosci.* **53**, 1040–1059 (2021).
53. Qian, Y., Yan, R. & Hu, S. Bearing degradation evaluation using recurrence quantification analysis and kalman filter. *IEEE Trans. Instrum. Meas.* **63**, 2599–2610 (2014).
54. Bhui, P. & Senroy, N. Application of recurrence quantification analysis to power system dynamic studies. *IEEE Trans. Power Syst.* **31**, 581–591 (2015).
55. Li, X., Ouyang, G., Yao, X. & Guan, X. Dynamical characteristics of pre-epileptic seizures in rats with recurrence quantification analysis. *Phys. Lett. A* **333**, 164–171 (2004).
56. Stender, M., Oberst, S., Tiedemann, M. & Hoffmann, N. Complex machine dynamics: Systematic recurrence quantification analysis of disk brake vibration data. *Nonlinear Dyn.* **97**, 2483–2497 (2019).
57. Collaboration, E. R. F. et al. C-reactive protein concentration and risk of coronary heart disease, stroke, and mortality: An individual participant meta-analysis. *Lancet* **375**, 132–140 (2010).
58. Bucciantini, M. et al. Inherent toxicity of aggregates implies a common mechanism for protein misfolding diseases. *Nature* **416**, 507–511 (2002).
59. Li, Z., Bianco, S., Zhang, Z. & Tang, C. Generic properties of random gene regulatory networks. *Quant. Biol.* **1**, 253–260 (2013).
60. Widder, S., Schicho, J. & Schuster, P. Dynamic patterns of gene regulation i: simple two-gene systems. *J. Theor. Biol.* **246**, 395–419 (2007).
61. Pomeau, Y. & Manneville, P. Intermittent transition to turbulence in dissipative dynamical systems. *Commun. Math. Phys.* **74**, 189–197 (1980).
62. Kumarasamy, S. *et al.* Extreme events and extreme multistability in a nearly conservative system. *Chaos: An Interdiscip. J. Nonlinear Sci.* **34**, 071103 (2024).
63. Marwan, N., Romano, M. C., Thiel, M. & Kurths, J. Recurrence plots for the analysis of complex systems. *Phys. Rep.* **438**, 237–329 (2007).
64. Ngamga, E. et al. Recurrence analysis of strange nonchaotic dynamics. *Phys. Rev. E* **75**, 036222 (2007).
65. Yu, P., Nie, Q., Tang, C. & Zhang, L. Nanog induced intermediate state in regulating stem cell differentiation and reprogramming. *BMC Syst. Biol.* **12**, 1–13 (2018).
66. Parikshak, N. N., Gandal, M. J. & Geschwind, D. H. Systems biology and gene networks in neurodevelopmental and neurodegenerative disorders. *Nat. Rev. Genet.* **16**, 441–458 (2015).
67. Guo, S. Linking genes to brain, behavior and neurological diseases: What can we learn from zebrafish?. *Genes Brain Behav.* **3**, 63–74 (2004).

Acknowledgements

S.V. would like to thank SRM IST, Ramapuram, India, for their financial support, vide number SRM/IST-RMP/

RI/004. S.K. thanks Easwari Engineering College, Tamil Nadu, India, for their financial support, vide number SRM/EEC/RI/006. T.K. and S.L.K. have been supported by the National Science Centre, Poland, OPUS Programs (Projects No. 2018/29/B/ST8/00457, and 2021/43/B/ST8/00641).

Author contributions
All the authors equally contributed to this paper.

Declarations

Competing interests
The authors declare no competing interests.

Additional information
Supplementary Information The online version contains supplementary material available at https://doi.org/10.1038/s41598-025-97268-w.

Correspondence and requests for materials should be addressed to S.L.K. or S.K.

Reprints and permissions information is available at www.nature.com/reprints.

Publisher's note Springer Nature remains neutral with regard to jurisdictional claims in published maps and institutional affiliations.